Estimating the impact of school closures on COVID-19 disease burden

Supplementary Appendix

——— Add Authors List here ———

Contents

1 Model description

1.1 General approach

We use a semi-mechanistic compartmental model of COVID-19 transmission governed by ordinary differential equations (ODEs). Our model captures important factors of COVID-19 transmission and disease such as age-specific characteristics, heterogeneous mixing, vaccination and the emergence of different variants of concern. The ODE-based model is used to capture only states relevant to transmission, whereas hospitalisations and deaths are estimated through a convolution process. This process combines the model-estimated disease incidence with statistical distributions modelling the time to hospitalisation, the hospital stay duration and the time to death. This approach presents two main advantages. First it reduces the complexity of the dynamic system relying on numerical solving of ODEs, which is computationally expensive. Second, the convolution approach allows for more flexibility and produces more realistic assumptions regarding the timings of hospitalisations and deaths, compared to what could be achieved with a simple compartmental approach. The following sections describe the model in details and Figure S1 summarises the overall approach used in our analysis.

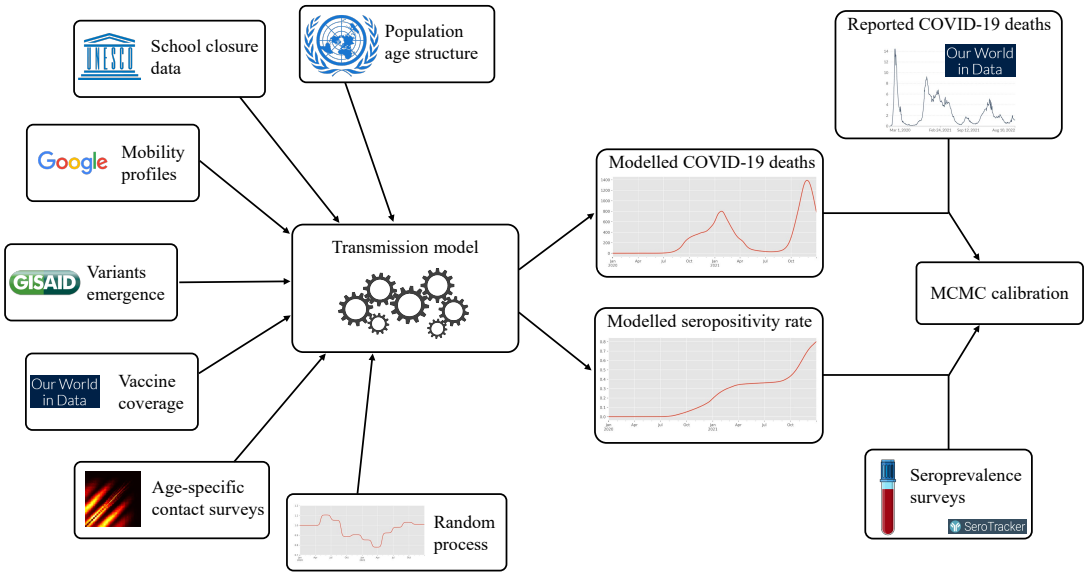

Figure S1: Conceptual approach used to build and calibrate the models

1.2 Transmission model

1.2.1 Compartment types and sequence

Model compartments represent sequential progressions through the processes of infection with, progression through, and recovery from the phases of SARS-CoV-2 infection and COVID-19 disease. The following types of compartments are implemented:

- Susceptible
  - Persons never previously infected with SARS-CoV-2 during or before the model simulation period
- Latent
  - Persons recently infected with SARS-CoV-2, but not in the active phase of the disease yet.
  - These individuals may still be infectious (see details in next paragraph).
- Active

  - Persons with active COVID-19 who are currently infectious.

- Recovered
  - Persons recovered from COVID-19 during the model simulation period
  - Reinfection from these compartments is permitted through exposure to a different strain than the one that most recently infected the individual (see strain stratification section for details).

The base model structure consists of a sequence of one susceptible compartment (S), four latent compartments (E_1, ..., E_4), four active disease compartments (I^1, ..., I^4) and one recovered compartment (R) (Figure S2).

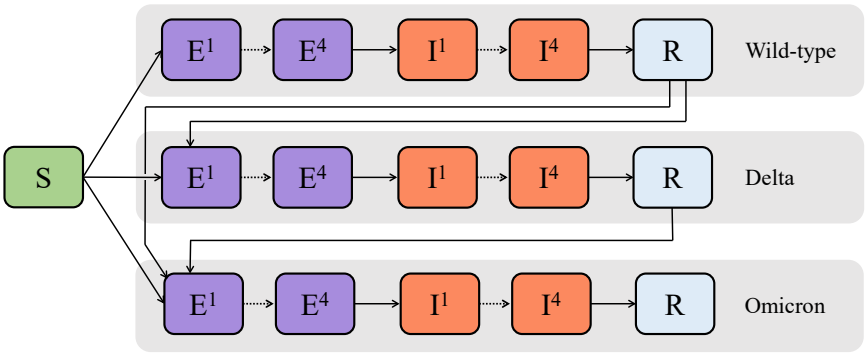

Figure S2: Compartmental model structure. S = Susceptible, E = Exposed / Latent, I = Active disease, R = Recovered. Stratification by age and vaccination status are not shown here.

The main rationale for using four serial compartments for both the latent and active states is to achieve an Erlang distribution for the time spent in each of these states. This distribution is more realistic than the exponential distribution that would have been associated with a single compartment, because the Erlang distribution does not have a large density mass around 0 and is not heavy-tailed. Figure S3 illustrates the modelled distributions of the incubation period and the active disease period.

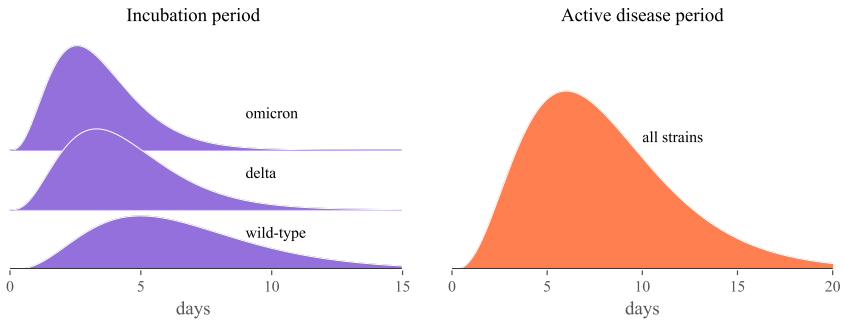

Figure S3: Modelled distributions of the incubation and active disease periods.

The four active disease compartments all have exactly the same characteristics. However, the last two latent compartments (E^3 and E^4) are infectious whereas the first two (E^1 and E^2) are not. We further assume that the infectious latent compartments are half as infectious as the active disease compartments.

1.2.2 Model stratification by age

All compartments of the base compartmental structure are stratified by age into the following age bands: zero to 14 years / 15 to 24 years / 25 to 49 years / 50 to 69 years / 70 years and above.

The initial population is distributed between the different age bands to reflect the age distributions reported by the United Nations Population Division. Demographic processes, including births, ageing and non-infection-related deaths are not simulated, given the timeframes considered in this simulation.

We assume heterogeneous mixing between the different age groups to account for the assortative nature of social interactions by age (see Section 1.2.5). Age is assumed to affect:

- The susceptibility to infection
- The risk of COVID-19 hospitalisation
- The risk of COVID-19 death
- The vaccination rate (see Section 1.2.3)

1.2.3 Capturing the effects of vaccination

History of vaccination is captured by stratifying all model compartments by vaccination status. Two vaccination strata are included to represent those who have received at least two doses of a COVID-19 vaccine, and those who have not.

We use data from *Our World in Data* to inform the modelled dynamic vaccination coverage. In particular, we use the reported proportion of people "fully vaccinated" to specify the time-variant proportion of vaccinated people in our model. We assume that older individuals are vaccinated first by prioritising the modelled age groups in descending order. That is, the oldest age group receives all available vaccines until a saturation coverage of 80% is reached for this group. Then the next oldest category starts receiving vaccines and we repeat this process until all available vaccines are allocated. Note that in the event that the population-level vaccine coverage exceeds 80%, the saturation coverage is set equal to the population-level coverage.

Let us consider two successive time points t_i and t_{i+1} for which vaccination data is available. Let us denote $r_{a,i}$ and $r_{a,i+1}$ the associated vaccine coverage for age group a. The time-variant and age-specific vaccination rate per capita $w_a(t)$ verifies:

$$1 - r_{a,i+1} = (1 - r_{a,i})e^{-w_a(t)(t_{i+1}-t_i)} \quad ,\forall t \in [t_i, t_{i+1}). \tag{1}$$

Then,

$$w_a(t) = \frac{\ln(1 - r_{a,i}) - \ln(1 - r_{a,i+1})}{t_{i+1} - t_i} \quad ,\forall t \in [t_i, t_{i+1}), \tag{2}$$

where $\ln(x)$ represents the natural logarithm of x.

WE COULD ADD A FIGURE HERE SHOWING MODELLED COVERAGE OVER TIME VS DATA FOR ALL COUNTRIES

The effect of vaccination on transmission is to partially reduce the rate of infection for all persons at-risk of infection in the vaccinated stratum. This includes both fully susceptible (never previously infected) persons, as well as recovered persons who are at risk of reinfection. The model allows for hybrid immunity in the sense that the vaccination-induced relative reduction of transmission risk is multiplied with that induced by previous infection. Vaccination is also assumed to reduce the risk of hospitalisation and death

Emerging variants of concern (VoCs) may partially escape vaccine-induced (as well as infection-induced) immunity, as described further below (see Section / Table XX).

1.2.4 Modelling multiple viral strains

The model is stratified by "strain" to simulate the emergence of multiple variants of concern (VoC). This approach explicitly represents multiple competing strains, each with a separate force of infection calculation. We assume that VoCs can have different levels of transmissibility, incubation period's duration and disease severity (hospitalisation and death risks) compared to the ancestral COVID-19 strain. In addition, VoCs are assumed to escape immunity partially for both vaccination- and infection-related immunity. The parameters used to represent the VOCs' characteristics are presented in Table XXX.

Seeding of each new strain into the model is achieved through the importation of a small number (10 per million population) of new infectious persons with the relevant strain into the model. The seeding process is done over a ten-day period and the start of this period is set between 30 days before and 30 days after the emergence date as reported by GISAID Table XXX. The exact start date is automatically calibrated by the MCMC algorithm.

1.2.5 Dynamic social mixing

The model captures changes in social interactions over time through a dynamic age-specific mixing matrix. The following sections describe how this matrix is defined and how it captures the different non-pharmaceutical interventions implemented in the analysed countries, including school closures.

1.2.5.1 Reference mixing matrices

We extracted country-specific contact matrices using the *socialmixr* R package (version 0.1.8) which derives social mixing matrices from contact survey data. These matrices provide the average numbers of contacts per day between different age groups, disaggregated by the following locations: home, school, work, other locations. We considered only the surveys conducted before the COVID-19 pandemic in order to obtain raw contact rate estimates that are not affected by COVID-19-related mobility changes. The next sections describe how we then adjusted the raw matrices to account for dynamic mobility.

For countries where contact survey data were not available, we used the matrices from a reference country among those with available data (Still need to come up with a plan for this). The reference matrices were then adjusted to account for age distribution differences between the modelled country and the reference country. For each location $L \in \{$"home", "school", "work", "other locations"$\}$ the age-specific contact matrix of the modelled country $C^L = (c^L_{i,j}) \in R_+^{5\times5}$ is defined such that $c^L_{i,j}$ is the average number of contacts that a typical individual aged i has with individuals aged j. Let us denote $Q^L = (q^L_{i,j}) \in R_+^{5\times5}$ the original matrix associated with location L for the reference country, where $q^L_{i,j}$ is defined using the same convention as for $c^L_{i,j}$. Let π_j denote the proportion of people aged j in the modelled country in 2020, and ρ_j the proportion of people aged j in the reference country at the time of the contact survey. The contact matrices C^L were obtained from:

$$c^L_{i,j} = q^L_{i,j} \times \frac{\pi_j}{\rho_j}. \tag{3}$$

The overall contact matrix (before adjustments for mobility changes) results from the summation of the four location-specific contact matrices: $C_0 = C_H + C_S + C_W + C_L$, where C_H, C_S, C_W and C_L are the age-specific contact matrices associated with households, schools, workplaces and other locations, respectively.

1.2.5.2 Modifications of contact rates over time

To capture mobility changes over time, the contributions of the matrices C_S, C_W and C_L vary with time such that the input contact matrix can be written:

$$C(t) = C_H + s(t)^2 C_S + w(t)^2 C_W + l(t)^2 C_L \tag{4}$$

The modifying functions s (for schools), w (for work) and l (for other-locations) are each squared to capture the effect of the mobility changes on both the infector and the infectee in any given interaction that could potentially result in transmission.

School closure/re-opening

Reduced attendance at schools is represented through the function s, which represents the proportion of all school students currently attending on-site teaching. If schools are fully closed at time t, $s(t) = 0$ and C_S does not contribute to the overall mixing matrix $C(t)$. The function s is derived from the UNESCO database on school closures since the start of the COVID-19 pandemic (ADD REF HERE). This database provides school opening status over time as a categorical variable taking the following values: "Fully open", "Partially open", "Academic break", "Closed due to COVID-19". Table S1 indicates how the different categorical values are converted into the numerical function s.

We included uncertainty around the value associated with the partial closure category, as there is no quantitative data available to inform this parameter. The partial closure periods are likely to be periods where only a small fraction of students such as children of "essential workers" were attending school. We assume that between 10 and 30% of students attended on-site learning during these periods.

To model the counterfactual "no school closure" scenario, we assume that the schools were "Fully open" during the periods reported as "Partially open" or "Closed due to COVID-19".

Figure S4 summarises the UNESCO data on school closure for the analysed countries.

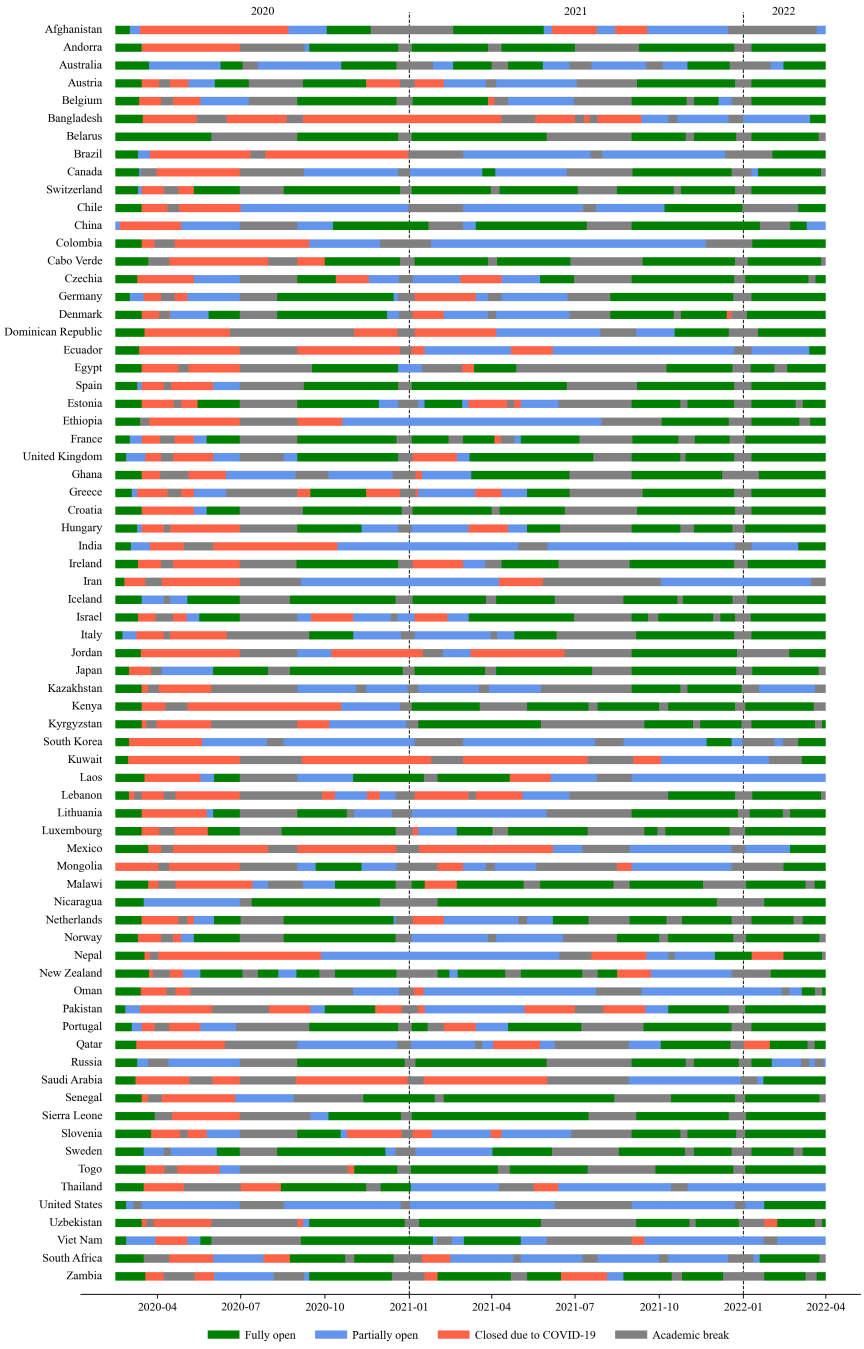

Figure S4: UNESCO data on school closures during the COVID-19 pandemic.

UNESCO category	Assumed proportion of students on-site ($s(t)$)
Fully open	100%
Partially open	10-30%
Academic break	0%
Closed due to COVID-19	0%

Table S1: Assumed percentage of students on-site for the different UNESCO school closure categories.

Dynamic mobility outside of schools and homes

Changes to people's mobility in places other than schools and homes are modelled using Google Mobility data. We use the "Workplace" category of the Google data to scale the work-related matrix contribution C_W to overall mixing over time, using the adjusting function w. The "other locations" matrix C_L is scaled through the adjusting function l which is defined as the average of the Google mobility indicators across the following Google categories: "Retail and recreation", "Grocery and pharmacy" and "Transit stations".

Household contacts

The contribution of household contacts to the overall mixing matrix is fixed over time. Although Google provides mobility estimates for residential contacts, the nature of these data is different from that of each of the other Google mobility types. They represent the time spent in that location, as opposed to other categories, which measure a change in total visitors rather than the duration. The daily frequency with which people attend their residence is likely to be close to one and we considered that household members likely have a daily opportunity for infection with each other household member regardless of the background level of mobility. Therefore, we did not implement a function to scale the contribution of household contacts to the mixing matrix with time.

1.2.6 Random transmission adjustment

The risk of SARS-CoV2 transmission per contact is adjusted by a time-variant random process, making the model semi-mechanistic. This random process reflects the fact that all the variations observed in the transmission risk in the real world cannot be explained solely by the factors that are included explicitly in the model such as vaccination, dynamic mobility or new variants' emergence. We therefore allow for random perturbations to the risk of transmission over time, although these perturbations are highly auto-correlated to avoid significant changes over a short period of time.

We use a random walk with gaussian update defined by:

$$\begin{aligned} W(0) &= 0 \\ W(t+1) &\sim \mathcal{N}(W(t), \epsilon) \quad , \end{aligned} \tag{5}$$

where $\mathcal{N}$ denotes the normal distribution and where the standard deviation ϵ is automatically calibrated by the MCMC. The random process W is updated on a fortnightly basis and is transformed using the exponential function before being applied to the risk of transmission per contact (see Equation 7).

1.2.7 Ordinary differential equations

Let us first introduce some new notations. The different age groups are indicated by the subscript a and $\mathcal{A}$ represents the set of all modelled age groups (see Section 1.2.2). The vaccination status is represented by the subscript v and $\mathcal{V}$ is the set of vaccination statuses (i.e. $\mathcal{V} = \{$"0", "1"$\}$ where "0" represents unvaccinated people and "1" represents vaccinated people). The subscript s is used to represent the different viral strains and $\mathcal{S}$ is the set of all strains (i.e. $\mathcal{S} = \{$"wild-type", "delta", "omicron"$\}$). The average incubation period duration associated with strain s is denoted q_s and the average duration of active disease is denoted w. The relative susceptibility to infection of individuals aged a with vaccination status v is denoted $\sigma_{a,v}$. The term $b_{a,v,s}(t)$ is used to designate the imported individuals of age a and with vaccination status v that are infected with strain s (infection seeding). Vaccination is characterised by the age-specific and time-variant per-capita vaccination rate w_a. Finally, $\chi_{s,\sigma}$ represents the relative susceptibility to infection with strain σ for individuals whose most recent infection episode was with strain

s. Using these new notations combined with those previously introduced, we can describe the model with the following set of ordinary differential equations:

$$\begin{aligned}
\frac{dS_{a,v}}{dt} &= -\sum_{s\in\mathcal{S}} \lambda_{a,s}(t)\sigma_{a,v}S_{a,v} + \Phi_v\omega_a(t)S_{a,v=0} \quad , \\
\frac{dE^1_{a,v,s}}{dt} &= \lambda_{a,s}(t)\sigma_{a,v}\Big(S_{a,v} + \sum_{\sigma\in\mathcal{S}} \chi_{\sigma,s}R_{a,v,\sigma}\Big) - \frac{4}{q_s}E^1_{a,v,s} + \Phi_v\omega_a(t)E^1_{a,v=0,s} \quad , \\
\frac{dE^k_{a,v,s}}{dt} &= \frac{4}{q_s}E^{k-1}_{a,v,s} - \frac{4}{q_s}E^k_{a,v,s} + \Phi_v\omega_a(t)E^k_{a,v=0,s} \quad , \forall k \in \{2,3,4\}, \\
\frac{dI^1_{a,v,s}}{dt} &= \frac{4}{q_s}E^4_{a,v,s} - \frac{4}{w}I^1_{a,v,s} + b_{a,v,s}(t) + \Phi_v\omega_a(t)I^1_{a,v=0,s} \quad , \\
\frac{dI^k_{a,v,s}}{dt} &= \frac{4}{w}I^{k-1}_{a,v,s} - \frac{4}{w}I^k_{a,v,s} + \Phi_v\omega_a(t)I^k_{a,v=0,s} \quad , \forall k \in \{2,3,4\}, \\
\frac{dR_{a,v,s}}{dt} &= \frac{4}{w}I^4_{a,v,s} - \sum_{\sigma\in\mathcal{S}} \lambda_{a,\sigma}(t)\sigma_{a,v}\chi_{s,\sigma}R_{a,v,s} + \Phi_v\omega_a(t)R_{a,v=0,s} \quad ,
\end{aligned} \tag{6}$$

where $\lambda_{a,s}$ represents the force of infection of strain s affecting individuals of age a. The quantity Φ_v is a binary variable used to switch between plus and minus signs depending on the vaccination status. It is equal to 1 when $v =$"1" and -1 when $v =$"0". In other words, $\Phi_v = 2\mathbb{1}_{v=\text{"1"}} - 1$.

The force of infection is calculated as:

$$\lambda_{a,s}(t) = \beta e^{W(t)}\rho_s \sum_{\alpha\in\mathcal{A}}\sum_{v\in\mathcal{V}} c_{a,\alpha}(t)\Big(0.5\sum_{k=3}^{4} E^k_{\alpha,v,s} + \sum_{k=1}^{4} I^k_{\alpha,v,s}\Big) \quad . \tag{7}$$

In the previous equation, β represents the unadjusted risk of transmission per contact and ρ_s is the relative transmissibility of strain s.

1.3 Estimation of COVID-19-related hospital pressure and deaths

The transmission model described in Section 1.2 provides estimates of COVID-19 incidence over time, disaggregated by age, vaccination status and strain. We combine these incidence estimates with the age-, vaccination- and strain-specific risks of hospitalisation and deaths as well as statistical distributions of time to events to compute COVID-19-related hospital pressure and deaths over time.

1.3.1 COVID-19-related hospital pressure

The risk of hospitalisation given infection is expected to vary dramatically by setting. For example, different countries may have different criteria for whether or not a COVID-19 patient should be admitted to a hospital. This makes it difficult to provide accurate estimates of hospitalisation rates for multiple countries.

This is why we introduce a universal indicator named "hospital pressure" in our analysis. This indicator is obtained by considering the age-specific risk of hospitalisation given infection observed in the first year of the pandemic in the Netherlands, adjusted for vaccination status and for the infecting strain (See Table XX). The "hospital pressure" indicator can therefore be interpreted as the level of hospital occupancy that would be observed in the analysed country if the rates of hospitalisation given infection in this country were the same as in the Netherlands. This indicator is expected to be approximately proportional to the actual hospital occupancy level of the studied country. Note that this indicator is used in order to make comparisons between scenarios such that one should interpret the relative differences between scenarios rather than the absolute values of the indicator.

Let us denote $i_{a,v,s}(t)$ the number of new disease episodes estimated to start at time t for people aged a with vaccination status v and infected with strain s. The number of new hospital admissions occurring at time t is calculated using the following convolution product:

$$\eta(t) = \sum_{a,v,s} \kappa_{a,v,s} \int_{u\geq 0} i_{a,v,s}(t-u)g_h(u)du \quad , \tag{8}$$

where $\kappa_{a,v,s}$ is the risk of hospitalisation given infection for age a, vaccination status v and strain s based on the Netherlands data, and g_h is the probability density function of the statistical distribution chosen to represent the time from symptom onset to hospitalisation (See Table XX).

We then compute the "hospital pressure" quantity h, which is an indicator of hospital occupancy level, by combining the number of new hospital admissions η with the statistical distribution used to model hospital stay duration:

$$h(t) = \int_{u \geq 0} \eta(t-u)(1-\tau(u))du \quad , \tag{9}$$

where τ is the cumulative density function of the statistical distribution chosen to represent the hospital stay duration (See Table XX).

1.3.2 COVID-19 deaths

We estimate the number of COVID-19 deaths over time using a similar approach as for the hospital pressure indicator. We use the age-specific infection fatality rates reported in ODriscoll et al. [2], adjusted for vaccination status and for the infecting strain to estimate COVID-19 mortality. Using the same notations as in Section 1.3.1, the number of COVID-19 deaths observed at time t is obtained by:

$$\mu(t) = m_C \sum_{a,v,s} ifr_{a,v,s} \int_{u \geq 0} i_{a,v,s}(t-u) g_d(u) du \quad , \tag{10}$$

where $ifr_{a,v,s}$ is the risk of death given infection for age a, vaccination status v and strain s, and g_d is the probability density function of the statistical distribution chosen to represent the time from symptom onset to death (See Table XX). We use a country-specific adjuster m_C to capture the fact that the infection fatality ratio is expected to vary by country, in part due to differences in COVID-19 death definition and reporting standards. This adjustment is automatically calibrated by the MCMC (Section 2).

2 Model calibration and uncertainty propagation

REVISE THE SECTION BELOW WHEN FINALISED The model was calibrated using a Bayesian approach. In particular, we used the adaptive Metropolis algorithm introduced by Haario *et al.* to sample parameters from their posterior distributions [1]. For each country, we ran 8 independent Metropolis chains initialised using Latin Hypercube Sampling based on the parameter priors. We ran simulations for X hours per chain in order to achieve at least 50,000 iterations per chain. We discarded the first 25,000 iterations of each chain as burn-in and combined the samples of the 8 chains to project epidemic trajectories over time. For each modelled country, the epidemic projections presented in our analysis are associated with 1000 parameter sets randomly sampled from the posterior distributions obtained from MCMC sampling. The definitions of the prior distributions and the likelihood are detailed in the following sections.

2.1 Parameters varied during calibration

The parameters varied during calibration along with their associated prior distributions are listed in Table (add ref to table here) and indicated with the superscript ^{c}. We used uniform prior distributions for all calibrated parameters. The primary parameters varied during calibration are the unadjusted risk of transmission per contact (β), the IFR multiplier (m_C), the infection seeding times of each strain and the proportion of students on-site during "Partially open" periods. Note that the values of the random process W_t described in Section 1.2.6 are also treated like calibrated parameters by the MCMC. They are associated with an improper uniform prior distribution, whereas the auto-regressive component described in Equation 5 is incorporated in the posterior likelihood computation (Section 2.3).

2.2 Calibration targets

For each country model calibration is achieved by targeting two COVID-19 burden indicators: the reported number of COVID-19 deaths over time and country-level seroprevalence estimates.

We used the daily number of COVID-19 deaths reported by Our World in Data and applied a 7-day moving average to the observed data. We used the online platform SeroTracker to extract country-specific seroprevalence estimates. Use Angus' description here.

2.3 Likelihood definition

Let d_w denote the rounded average daily number of COVID-19 deaths during week w, and $\hat{d_w}^{\theta}$ the associated predicted number of deaths according to the model with parameter set θ.

Let us denote m the sample size associated with the seroprevalence survey selected from SeroTracker (Section 2.2), and k the number of seropositive individuals observed in the survey. Let $\hat{\pi}^{\theta}$ denote the modelled proportion ever infected by the time the survey was conducted (using midpoint date) associated with the parameter set θ. The likelihood was defined as follows:

$$\mathcal{L}(\theta) := f_{m,\hat{\pi}^{\theta}}(k) \times \prod_{w} g_r(d_w | \hat{d_w}^{\theta}) \quad , \tag{11}$$

where $f_{n,p}(.)$ is the probability mass function of a binomial distribution $\mathcal{B}(n,p)$, and $g_r(.|\mu)$ is the probability mass function of a negative binomial distribution with mean μ and overdispersion parameter r. The parameter r is automatically estimated by the MCMC algorithm.

The likelihood described above represents the goodness of fit of a particular model parameterisation with regards to the targeted data. This quantity needs to be adjusted for the prior likelihood of the parameter set in order to compute the MCMC acceptance quantity $\mathcal{Q}(\theta)$. As we used uniform priors for all the parameters, the inclusion of the individual parameters' priors in the acceptance quantity is not necessary. Indeed, their respective contributions would cancel out as the same quantity would appear in the numerator and the denominator of the MCMC acceptance quantity ratio. However, the autoregressive relationship described in Equation 5 must be accounted for as part of the combined prior likelihood of a parameter set. This is what prevents unrealistic fluctuations of the random process. If W^{θ} represents the random process associated with the parameter set θ, the overall MCMC acceptance quantity is obtained by:

$$\begin{aligned} \mathcal{Q}(\theta) &= \mathcal{L}(\theta) \times \prod_{i=1}^{n} z_{W_{i-1}^{\theta},\sigma}(W_i^{\theta}) \\ &= f_{m,\hat{\pi}^{\theta}}(k) \times \prod_{w} g_r(d_w | \hat{d_w}^{\theta}) \times \prod_{i=1}^{n} z_{W_{i-1}^{\theta},\sigma}(W_i^{\theta}) \quad , \end{aligned} \tag{12}$$

where $z_{\mu,\sigma}(.)$ represents the probability density function of the normal distribution $\mathcal{N}(\mu,\sigma)$, and n is the number of random process updates. The standard deviation σ is automatically estimated by the MCMC.

2.4 Model coding and run time

NEED TO COMPLETE THIS. Maybe David can help here? Can probably find a better title for this section... Describe the following aspects here:

1. Model is complex
2. Need numerous model evaluations for calibration
3. Random process makes calibration even more challenging (large dimension)
4. Describe the solution:
   (a) Conceptual Approach to coding
   (b) Version control / Code availability

(c) Jax magic

5. Resulting average run time per model evaluation

References

[1] Heikki Haario, Eero Saksman, and Johanna Tamminen. "An adaptive Metropolis algorithm". In: *Bernoulli* 7.2 (2001).

[2] M. O'Driscoll et al. "Age-specific mortality and immunity patterns of SARS-CoV-2". In: *Nature* 590.7844 (2021), pp. 140–145. ISSN: 1476-4687. DOI: 10.1038/s41586-020-2918-0. URL: https://www.ncbi.nlm.nih.gov/pubmed/33137809.